

# Estimating Contact Force Rate Using Skin Deformation Cues

Bingxu Li<sup>1</sup> ✉, Gregory J. Gerling<sup>2</sup>, and Tyler Cody<sup>1</sup>

<sup>1</sup> SmartHap, Charlottesville, Virginia, USA

<sup>2</sup> University of Virginia, Charlottesville, Virginia, USA  
bingxu.contact@gmail.com

**Abstract.** Knowledge of contact force is important in various fields as it provides essential insights into the interactions between objects. Understanding the forces exerted during human-machine interactions is essential for optimizing performance and preventing discomfort or injury. Despite the significance of contact force, there are limited approaches for estimating it accurately when direct measurements are not available. Existing methods often come with constraints such as complexity, cost, and environmental limitations. This paper introduces a method for estimating contact force from skin deformation cues in bare-finger interactions using linear regression models. The statistical results from the linear models align with scientific studies, revealing a significant correlation between force and skin deformation that has a dependence on stimulus moduli. The developed models exhibit reliable estimations of force, with robustness to variances between trials and insensitivity to individual differences in skin properties. This approach offers an alternative method for estimating contact force and indicates the potential of models for estimating key variables associated with user experience.

**Keywords:** Tactile Feedback · Contact Force Prediction · Human-Machine Interaction

## 1 Introduction

Tactile force, relating to sense of touch, becomes a critical consideration in minimizing tissue damage in surgical procedures [4, 22], facilitating responsive and adaptive capabilities in robotics and automation [16, 17], and enhancing realism and immersion in virtual environments [16, 19]. One way to measure force is to use stick-based tools designed with force sensors to provide feedback to the manipulator, commonly used in surgical robots and laparoscopic instrumentation for precision and safety control [3, 26]. Although this approach is suitable for tasks demanding fine control, it requires additional equipment or accessories, involves higher learning curves during user training, and results in unnatural interactions. On the other hand, bare-finger interaction offers a natural and intuitive way to interact with objects by eliminating the need for additional tools

and enabling users to perform multiple actions simultaneously. Many applications benefit from utilizing bare-finger interactions to optimize user experiences. The key challenge is limited force feedback to the user, attributed to the absence of sensors on the contact surface and the non-linear characteristics of the natural skin. For example, particularly in virtual and augmented reality (VR/AR) environments where realism and immersion are primary for user experience, the measurement of force becomes crucial but constrained because users often interact with virtual objects without physical touch. One method is to apply physics-based models by implementing physics engines that simulate the dynamics and interactions between virtual objects, but it has limitations including sensitivity to model parameters, computational complexity, and simplified contact models [1, 21, 29]. Another method is to use myography techniques, such as surface electromyography (sEMG), which outputs electric activity of conductive materials upon physical contact [5]. This technology is frequently used in biomechanical settings [7, 28] and human-computer interaction (HCI) applications to detect contact events [24, 30]. However, this method has limitations including electrode wiring and implementation, low spatial resolution, and sensitivity to electric and magnetic interference [8, 23]. In scenarios where the spaces or access is restricted, such as physical therapy, direct force assessment becomes impractical due to constraints of physical space and patient comfort. One common method is to use visual observation by tracking identified markers, carried out either by a dedicated hardware or a skilled individual [18, 21], but it shows limitations in quantitative data and its high dependence on visual cues.

Thus, in bare-finger interactions, these limitations associated the current approaches highlight the need for complementary methods including predictive models that can also serve as an indirect, albeit virtual, measurement of force. In tactile sensing, contact force rate, along with skin deformation cues, contributes to the psychophysical perception of an object’s compliance [11, 25]. This relationship is influenced both by the material properties of the objects and dynamic aspects of the interaction [27]. In this paper, we construct multivariate linear models using skin deformation cues as predictors and biomechanical measurements from previously published studies in passive touch [14]. Our results show that the developed models can predict contact force rate using skin deformation cues with maximum error less than a detection threshold of 0.08 N/s, a detection threshold found in previous studies [15].

The remainder of this paper is structured as follows. Next, we describe the data collection, measurement, and modeling methods. Then, we present our results. The paper concludes with a discussion of the results.

## 2 Methods

In previous research [10], we employed a custom-built imaging system that facilitates direct visualization of skin surface in the form of a 3-D point cloud, while the skin undergoes indentation of contact. In previous studies [13, 15], cues derived from the point cloud were used to quantify the spatial deformation of

skin surface. Biomechanical experiments were conducted across a group of participants, in which the relationship between contact force and skin deformation with varying stimulus moduli was evaluated. In the following, the relevant details of the imaging system and experiments are described and the data processing and model construction methods used in this paper are given.

## 2.1 Participants

A total of 25 participants (mean age = 27, range = 21 - 30; 11 males and 14 females) were recruited in the experiments, which all fully completed. The experiments were approved by the local Institutional Review Board, and informed consent was obtained from each participants. None had prior knowledge about the experiments and their fingers were free of calluses and scars. All devices and surfaces were sanitized after each use.

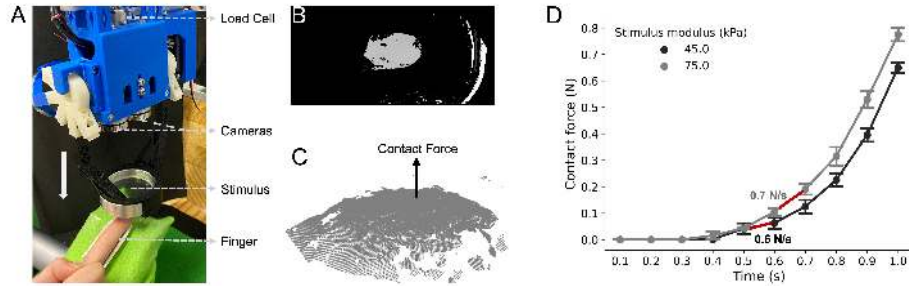


**Fig. 1. Experimental setup for observing skin deformation and measuring contact force.** (A) Mechanical-electrical indenter that delivers elastic stimulus to the fingertip. (B) One image of the fingertip captured by the right camera when indented by a 45 kPa stimulus. (C) Construction of a 3-D point cloud from captured images using disparity-mapping method. (D) Contact force is recorded simultaneously over an indentation of 1 second. The rate of force is calculated as 0.6 and 0.7 N/s for the 45 and 75 kPa stimulus, respectively. The segment in red indicates the median value of the intermediate change rates.

## 2.2 Apparatus

The apparatus [10] used for skin surface visualization, force measurement, and biomechanical experiments consists of a custom-built, electrical-mechanical motion indenter (ILS-100 MVTP, Newport, Irvine, CA, USA) paired with two stereo cameras and a load cell installed on a cantilever, shown in Fig.1A. Elastic stimuli are individually placed in a 3D printed rotatable housing, and each can be delivered to the fingertip at controlled rate and displacement. A support platform consists of a cylindrical, heavy duty aluminum rod attached with a rectangular aluminum hand rest was designed to stabilize the participant's finger at a 30-degree angle with respect the stimulus surface. The hand rest includes a rigid

plastic housing that holds the finger in position and helps minimizing subtle movements during experiments. An inclined 30-degree contact is chosen because of the high concentration of mechanoreceptors at the fingertip. The displacement of stimulus is recorded by the motion controlled with resolution of 0.001 mm, with force measured by the load cell (LCFD-5, Omegadyne, Sunbury, OH, USA) at a frequency of 150 Hz, with a resolution of  $\pm 0.05$  N. Images are captured by the left and right cameras (Papalook PA150, Shenzhen Aoni Electronic Industry Co., Guangdong, China) at 30 frames per second with maximum resolution of 1280 x 720 pixels, maintaining a manual focus during experiments. This custom-built imaging system shows competitive advantages in capturing high spatial resolution of the skin surface, facilitating direct visualization of skin dynamics in bare-finger interactions, and providing empirical measurements to characterize skin responses upon contact with elastic stimuli of varying compliance.

### 2.3 Skin Deformation Cues and Contact Force

Using the images collected by the cameras, a disparity-mapping method was applied for generating a 3-D point cloud that represents the geometry of skin surface, Fig.1B-C. To quantitatively characterize skin geometry, in prior work [14] we developed an ellipse fitting algorithm by fitting vertically stacked, uni-orientated ellipses to the point cloud, to derive mechanical cues that describe skin deformation over time. The skin deformation cues include contact area, curvature, eccentricity, and penetration depth.

The change rates of contact force and skin deformation cues are calculated and used in the statistical analysis, as rate-based cues describe both spatial and temporal aspects of dynamic changes of the skin, and are found to be associated with psychophysical responses [2, 13]. In the experiments, contact force was measured by the load cell when the fingertip was making contact with the stimulus. The change rate of force was determined as the median value of a sequence of intermediate rates calculated at every 0.1 second time interval. Fig.1D shows the change in force over an indentation by the 45 and 75 kPa stimulus, and their force rate was calculated as 0.6 and 0.7 N/s, respectively.

### 2.4 Biomechanical Experiments

Biomechanical measurements of skin deformation were conducted in passive touch. Two elastic stimuli were fabricated with moduli of 45 and 75 kPa. These moduli were chosen to closely approximate a slightly higher modulus than that of the skin at the fingertip [9]. During the experiments, the participants were seated in a comfortable chair with elbows resting on the table. Their index finger was stabilized and indented by the stimulus at 1.75 mm/s rate for 2 mm displacement. 3-D point clouds were generated at every 0.1 second during indentation, followed by acquisition of the skin deformation cues. Each stimulus was indented for 3 repeated repetitions. In total, there were 150 indentations

conducted in this experiments (25 participants, 2 stimuli, and 3 repetitions) and 1500 3-D point clouds generated.

## 2.5 Data Processing and Model Construction

The 1500 3-D point clouds were processed into 1500 instances of skin deformation cues, and then further processed into 150 instances of change rate of cues—one instance for each indentation. The median change rates of contact area, curvature, eccentricity, and penetration depth are the 4 predictors (referred to generally as skin deformation cues in the following) and the median change rate of contact force is the predicted response. The instances were divided by stimuli into two 75 instance samples, and then further split into 70% subsamples of 52 instances for training and 30% subsamples of 23 instances for testing.

Three linear regression models were assessed in this study: Ordinary Least Squares (OLS), Lasso, and Ridge regression. The mathematical formula used for multivariate OLS regression is:

$$y = \beta_0 + \beta_1x_1 + \dots + \beta_4x_4 + \epsilon \quad (1)$$

for multivariate Lasso regression is:

$$y = \beta_0 + \sum_{j=1}^4 \beta_jx_j + \lambda \sum_{j=1}^4 |\beta_j| \quad (2)$$

for multivariate Ridge regression is:

$$y = \beta_0 + \sum_{j=1}^4 \beta_jx_j + \lambda \sum_{j=1}^4 \beta_j^2 \quad (3)$$

where  $y$  is the dependent variable,  $x_1, x_2, \dots, x_4$  are the independent variables, and  $\beta_0, \beta_1, \dots, \beta_4$  are the regression coefficients.  $\epsilon$  is the error term in OLS regression model that minimizes the sum of squared residuals (SSE) to estimate the coefficients. In Lasso and Ridge regression, the  $L_1$  penalty  $\sum_{j=1}^4 |\beta_j|$  and the  $L_2$  penalty  $\sum_{j=1}^4 \beta_j^2$  are used to decrease coefficients to zero or near-zero, respectively, and the regularization term  $\lambda$  is a penalty parameter that controls the decrement. To construct the model, the change rates of four skin deformation cues were considered as the independent variables to predict contact force rate which is the dependent variable. The entire dataset was normalized before regression fitting. The hyper-parameter  $\lambda$  for Ridge and Lasso regression at each stimulus were determined by the GridSearch method through optimizing  $r^2$  score over a 10-fold cross-validation of their respective training subsamples. Subsequently, the linear models are constructed from the 52-instance training subsamples and tested by 23-instance testing subsamples.

### 3 Results

#### 3.1 The Relationship between Force and Skin Deformation Cues

The statistical correlations among the rate of change in skin deformation cues and their correlations with force rate were evaluated using the t-test for both the 45 and 75 kPa stimuli, as shown in Fig.2A-B. The results indicate two major findings. First, the cues show statistical independence, as reflected in low correlation values. Second, the correlation between force and skin deformation cues varies with stimulus modulus. In particular, force rate exhibited high correlations with the rate of contact area ( $r = 0.76$ ) and curvature ( $r = 0.7$ ) for the 45 kPa stimulus, Fig.2C; whereas it correlates with the rate of contact area ( $r = 0.71$ ) and eccentricity ( $r = 0.77$ ), for the 75 kPa stimulus, Fig.2D.

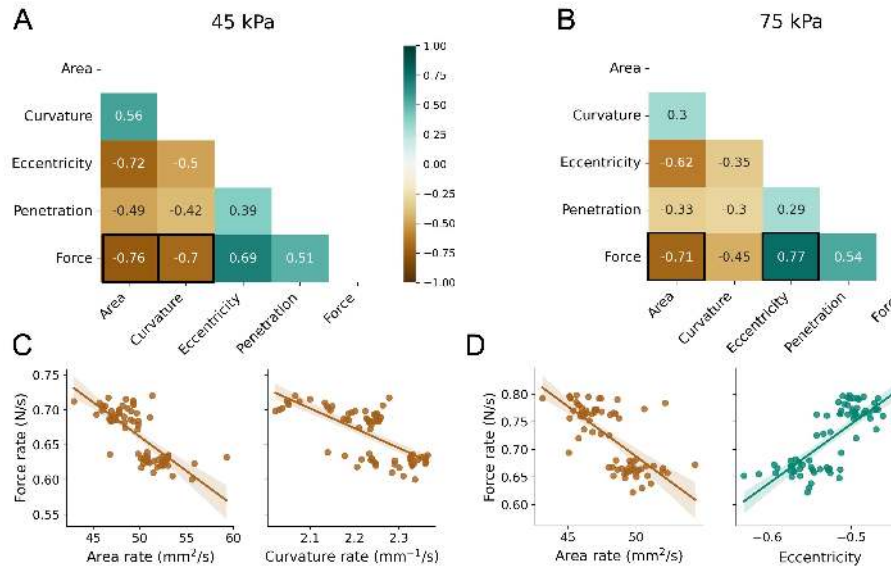


**Fig. 2. Statistical correlations between the rate of skin deformation cues and force.** The correlation values that higher than 0.7 are highlighted in a black frame for the (A) 45 kPa and (B) 75 kPa stimulus. Panel (C) and (D) present the overall data from 75 trials, indicating a high correlation between force rate with the rate of (C) contact area and curvature for the 45 kPa stimulus, and (D) contact area and eccentricity for the 75 kPa stimulus.

#### 3.2 Constructing Regression Models for Force Prediction

The correlation analysis depicted in Fig.2 suggests that the change rate of contract force can be predicted using the skin deformation cues. The prediction

results from the linear models using all four skin deformation cues as predictors are presented in Fig.3. The maximum error is calculated as the error mean plus two standard deviations. The results show that the OLS regression model yields the highest  $R^2$  value of 0.701, with a maximum error of 0.058 N/s for the 45 kPa stimulus; whereas the Ridge regression model achieves  $R^2$  value of 0.77, with a maximum error of 0.04 N/s for the 75 kPa stimulus. Notably, previous research found a force rate difference of 0.08 N/s between 45 and 75 kPa stimulus to not be differentiable by participants [13, 15]. This implies that while errors were observed in the regression model, the maximum error is significantly below the detection threshold. Moreover, a higher prediction performance is observed for the stiffer stimulus (75 kPa). This is because the change rate of force is more associated with stimuli that are To validate the linearity of the predictive relationship between the skin deformation cues and the change rate of force, a second-order polynomial regression analysis was conducted, which revealed a low coefficient ( $R^2 = 0.462$ , mean error =  $0.11 \pm 0.06$ ) implying a predominantly linear relationship.

	45 kPa		75 kPa	
Model	$R^2$ score	Max error	$R^2$ score	Max error
OLS	0.701	0.057894	0.765	0.04914
Ridge	0.692	0.059701	0.773	0.041797
Lasso	0.700	0.057616	0.761	0.047278

**Fig. 3. Results from the three regression models for force prediction** The optimal parameter used for the Ridge and Lasso regression was determined using Grid search method by the highest  $R^2$  score.

### 3.3 Significance of Skin Deformation Cues on Predicting Force

By using analyzing the Lasso regression models, we can compare the significance of each cue in predicting change rate of force. As part of the fitting process, Lasso regression increases and decreases the weight of predictors to optimize performance. The feature importance from the Lasso regression models are given in Fig.4 and show that the change rates of contact area and curvature are primary cues used for predicting force rate for the 45 kPa stimulus, whereas the change rates of eccentricity and penetration depth are the primary cues for the 75 kPa stimulus. This aligns with the correlations found in Fig.2.

To further validate the predictive significance of each cue, we conducted an analysis wherein the models were constructed by systematically excluding one cue at a time for force prediction. This approach allowed us to assess how much the model performance was affected by the excluded cue. The results are shown in Fig.5. For the 45 kPa stimulus, the results show a significant drop in model outcomes when the change rates of curvature and contact area were excluded from constructing the model, Fig.5A; whereas excluding the change rates of

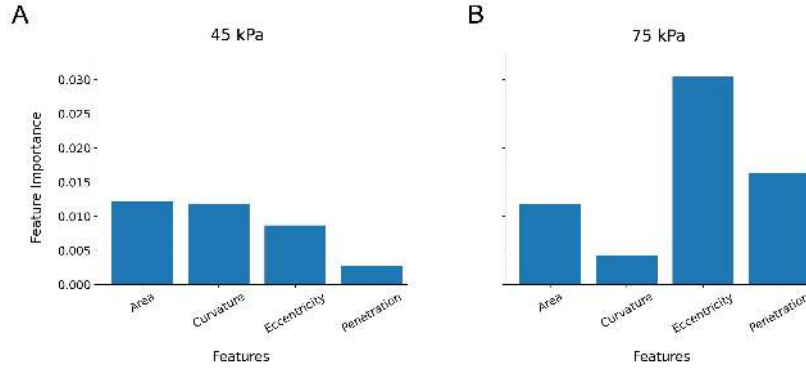


**Fig. 4. Significance of skin deformation cues in predicting contact force using Lasso regression.**

penetration depth and eccentricity resulted in a performance decrease in force prediction for the 75 kPa stimulus, Fig. 5B.

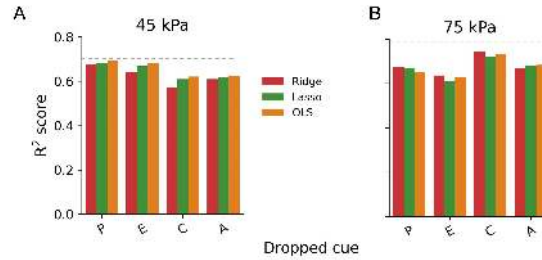


**Fig. 5. Validation of the impact of each cue in force prediction by constructing the models with only three cues.** The letter (P, E, C, A) on the x-axis indicates the corresponding cue that has been dropped. Letter P, E, C, A, represents: the change rate of penetration, eccentricity, curvature and area, respectively. The gray dash line indicates the  $R^2$  value when the model uses all four cues for prediction.

### 3.4 Effects of Sample Size, Stimulus Modulus, and Individual Differences on Force Prediction

The predictive capacity of the models may be influenced by various factors, including the training sample size, the modulus of tested stimuli, variances between trials, and also individual differences in skin properties and between skin states.

To assess the impact of sample size, we calculated  $R^2$  values using the regression models as the number of samples used for model training were incrementally increased, as shown in Fig. 6. The results indicate a minimum of 40 samples ( $n = 40$ ) is necessary for the models to achieve stability and optimal performance. Note that errors less than 0.08 N/s are considered not differentiable [13, 15]. We



can observe that for the 45 kPa stimulus errors are below the detection threshold at  $n = 29$ , as shown in Fig.6A, and for the 75 kPa stimulus at  $n = 26$ , as shown in Fig.6B. Overall, the models exhibit reduced errors and demand a smaller sample size for enhanced performance in the case of the stiffer stimulus.

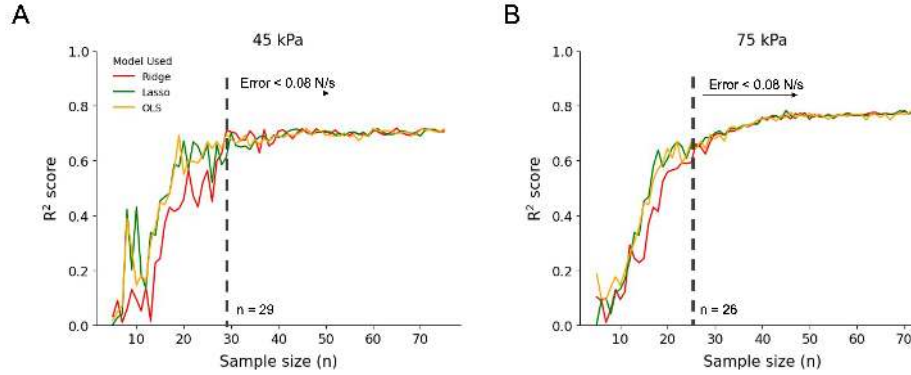


**Fig. 6. Evaluation of the impact of sample size on model performance ( $n = 75$ ).** Starting at  $n = 5$ , the models use 70% for training and 30% for testing. The dash line indicates the sample size at which the error falls below the detection threshold.

Additionally, we evaluated the model’s sensitivity to stimulus moduli by constructing a model using data from the 45 kPa stimulus and applied it to predict force rates for the 75 kPa stimulus, and vice versa, Fig.7. The results revealed a notable decline in performance for cross model prediction, with errors exceeding the detection threshold of 0.08 N/s. This underscores the necessity for distinct models used in predicting force regarding the stimulus moduli.

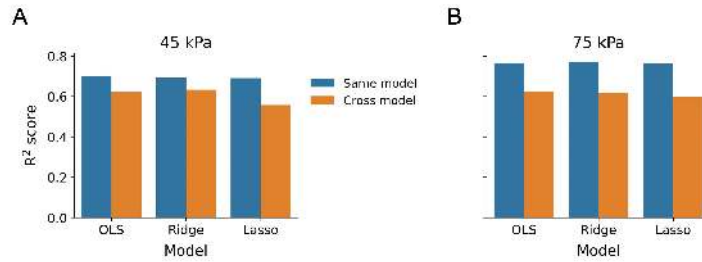


**Fig. 7. Validation of the distinctiveness of model for force prediction**(A) The model is fit with the data of 45 kPa stimulus making predictions for both 45 (same model) and 75 kPa (cross model) stimuli. Similarly, in (B) the model is fit with the data of 75 kPa stimulus.

Lastly, we investigated the influence of individual differences and variations between trials on the model capability in force prediction. The data of two participants, one with a soft and another with a stiffer index finger, was chosen for the analysis, Fig.8. Each participant underwent three experimental trials before and after skin modulation, in which their finger stiffness was manipulated by the application of hyaluronic acid at skin surface [13]. Regression models were used to predict force rate at each trial, which was compared with the actual values measured by the load cell, for the 45 and 75 kPa stimuli. The findings indicate consistent outcomes ( $R^2 = 0.74, 0.75$  for Participant A and B for the 45 kPa, and  $R^2 = 0.84, 0.82$  for Participant A and B for the 75 kPa, respectively) from the model for force prediction, with errors falling below the detection threshold ( $< 0.03$  N/s). This validates that the developed model is robust against variances between trials, and also insensitive to skin stiffness and changes in skin states.

## 4 Discussion

The main objective of this work was to develop models capable of predicting contact force using information from skin deformation cues. We constructed multivariate linear models for the change rate of contact force using the change rate of skin deformation cues as predictors. The models achieved a maximum error less than a detection threshold of 0.08 N/s. The threshold was determined through human-subject experiments conducted in [15], where the participants were asked to perceptually differentiate between the 45 and 75 kPa stimuli. Psychophysical results reveal that these two stimuli are not perceptually distinguishable ( $< 75\%$  correct rate). The observed difference in force rate was 0.08 N/s and the mean difference in force magnitude was 0.13 N at a stimulus indentation of 2 mm, is comparable with the just-noticeable difference (JND) of 0.1 N on the fingertips upon normal indentation [6, 12]. Another advantage of the developed models is the requirement of a relatively small number of samples for model training, as shown in Fig.6, as well as the models appear to be robust to variances between experimental trials and in skin properties, as shown in Fig.8.

The observed predictive importance of each cue is aligned with scientific findings [15, 20], showing that in tactile interaction, the change rate of contact area shows correlation with the change rate of contact force irrespective of stimulus moduli, whereas other cues exhibit such correlation depending on the stimulus moduli. This phenomena occurs because when indented by a soft stimulus, the finger tends to retain its shape which makes curvature stands out as a cue capturing spatial changes on skin surface; in contrast, when indented by a hard stimulus, the skin quickly flattens out at the contact surface, which makes eccentricity a stronger cue influencing contact force. This scientific understanding underscores and rationalizes the degradation in cross model performance shown in Fig.7.

In future work, it is important to consider the means of measuring skin deformation cues. The experimental apparatus used in this paper is designed

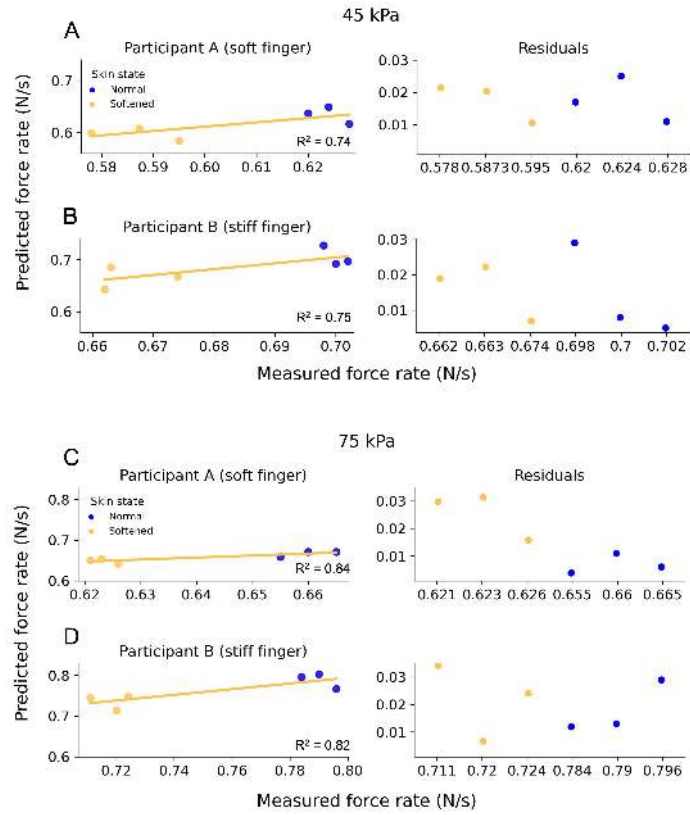


**Fig. 8. Evaluating the effects of between-trial variances, skin stiffness and modulation of skin state, on force prediction capability** Participant A with soft finger (stiffness = 0.1 N/mm) and Participant B with stiff finger (stiffness = 0.15 N/mm) were selected for the analysis. Ridge regression models were used to predict force rate and compared with the actual value measured by the load cell. (A) and (B) indicate the prediction performance for the two participants before and after their skin was softened by hyaluronic acid, for the 45 kPa stimulus, and (C) and (D) for the 75 kPa stimulus. The error (residual) from each prediction is reflected correspondingly on the right side.

for scientific purposes, has high spatial and temporal resolution, and involves complex mechanical systems. Alternative approaches may be more practical for engineered systems.

**Disclosure of Interests.** The authors claimed to have no interest of conflict

**Acknowledgments.** This work was supported in part by the National Science Foundation (IIS-1908115) and National Institutes of Health (R01NS105241, NCCIH R21AT011980, and U24AT011970)

## References

- [1] Abbiendi, G., collaboration, O., et al.: Tests of the standard model and constraints on new physics from measurements of fermion-pair production at 189-209 gev at lep. arXiv preprint hep-ex/0309053 (2003)
- [2] Ambrosi, G., Bicchi, A., De Rossi, D., Scilingo, E.P.: The role of contact area spread rate in haptic discrimination of softness. In: Proceedings 1999 IEEE International Conference on Robotics and Automation (Cat. No. 99CH36288C). vol. 1, pp. 305–310. IEEE (1999)
- [3] Autorino, R., Kaouk, J.H., Stolzenburg, J.U., Gill, I.S., Mottrie, A., Tewari, A., Cadeddu, J.A.: Current status and future directions of robotic single-site surgery: a systematic review. *European urology* **63**(2), 266–280 (2013)
- [4] Chen, E., Marcus, B.: Force feedback for surgical simulation. *Proceedings of the IEEE* **86**(3), 524–530 (1998). <https://doi.org/10.1109/5.662877>
- [5] Chowdhury, R.H., Reaz, M.B., Ali, M.A.B.M., Bakar, A.A., Chellappan, K., Chang, T.G.: Surface electromyography signal processing and classification techniques. *Sensors* **13**(9), 12431–12466 (2013)
- [6] Dahiya, R.S., Metta, G., Valle, M., Sandini, G.: Tactile sensing—from humans to humanoids. *IEEE transactions on robotics* **26**(1), 1–20 (2009)
- [7] De Luca, C.J.: The use of surface electromyography in biomechanics. *Journal of Applied Biomechanics* **13**(2), 135–163 (1997)
- [8] Disselhorst-Klug, C., Schmitz-Rode, T., Rau, G.: Surface electromyography and muscle force: Limits in semg–force relationship and new approaches for applications. *Clinical Biomechanics* **24**(3), 225–235 (2009)
- [9] Gerling, G.J., Hauser, S.C., Soltis, B.R., Bowen, A.K., Fanta, K.D., Wang, Y.: A standard methodology to characterize the intrinsic material properties of compliant test stimuli. *IEEE Transactions on Haptics* **11**(4), 498–508 (2018). <https://doi.org/10.1109/TOH.2018.2825396>
- [10] Hauser, S.C., Gerling, G.J.: Imaging the 3-D deformation of the finger pad when interacting with compliant materials. In: 2018 IEEE Haptics Symposium (HAPTICS). pp. 7–13. IEEE (2018)
- [11] Hirota, K., Ujitoko, Y., Sakurai, S., Nojima, T.: Deformation matching: Force computation based on deformation optimization. *IEEE Transactions on Haptics* **15**(2), 267–279 (2022). <https://doi.org/10.1109/TOH.2022.3142053>
- [12] LaMotte, R.H., Srinivasan, M.A.: Tactile discrimination of shape: responses of slowly adapting mechanoreceptor afferents to a step stroked across the monkey fingerpad. *Journal of Neuroscience* **7**(6), 1655–1671 (1987)
- [13] Li, B., Gerling, G.J.: An individual’s skin stiffness predicts their tactile discrimination of compliance. *The Journal of Physiology* (2023)
- [14] Li, B., Hauser, S., Gerling, G.J.: Identifying 3-D spatiotemporal skin deformation cues evoked in interacting with compliant elastic surfaces. In: 2020 IEEE Haptics Symposium (HAPTICS). pp. 35–40 (2020).

- <https://doi.org/10.1109/HAPTICS45997.2020.ras.HAP20.22.5a9b38d8>
- [15] Li, B., Hauser, S.C., Gerling, G.J.: Faster indentation influences skin deformation to reduce tactile discriminability of compliant objects. *IEEE Transactions on Haptics* **16**(2), 215–227 (2023). <https://doi.org/10.1109/TOH.2023.3253256>
  - [16] Magrini, E., Flacco, F., De Luca, A.: Estimation of contact forces using a virtual force sensor. In: 2014 IEEE/RSJ International Conference on Intelligent Robots and Systems. pp. 2126–2133 (2014). <https://doi.org/10.1109/IROS.2014.6942848>
  - [17] Magrini, E., Flacco, F., De Luca, A.: Control of generalized contact motion and force in physical human-robot interaction. In: 2015 IEEE International Conference on Robotics and Automation (ICRA). pp. 2298–2304 (2015). <https://doi.org/10.1109/ICRA.2015.7139504>
  - [18] Nakagaki, H., Kitagi, K., Ogasawara, T., Tsukune, H.: Study of insertion task of a flexible wire into a hole by using visual tracking observed by stereo vision. In: Proceedings of IEEE International Conference on Robotics and Automation. vol. 4, pp. 3209–3214. IEEE (1996)
  - [19] Park, J., Khatib, O.: A haptic teleoperation approach based on contact force control. *The International Journal of Robotics Research* **25**(5-6), 575–591 (2006)
  - [20] Pawluk, D.T., Howe, R.D.: Dynamic contact of the human fingerpad against a flat surface (1999)
  - [21] Pham, T.H., Kyriazis, N., Argyros, A.A., Kheddar, A.: Hand-object contact force estimation from markerless visual tracking. *IEEE Transactions on Pattern Analysis and Machine Intelligence* **40**(12), 2883–2896 (2017)
  - [22] Puangmali, P., Althoefer, K., Seneviratne, L.D., Murphy, D., Dasgupta, P.: State-of-the-art in force and tactile sensing for minimally invasive surgery. *IEEE Sensors Journal* **8**(4), 371–381 (2008). <https://doi.org/10.1109/JSEN.2008.917481>
  - [23] Pylatiuk, C., Muller-Riederer, M., Kargov, A., Schulz, S., Schill, O., Reischl, M., Bretthauer, G.: Comparison of surface emg monitoring electrodes for long-term use in rehabilitation device control. In: 2009 IEEE International Conference on Rehabilitation Robotics. pp. 300–304. IEEE (2009)
  - [24] Qi, J., Jiang, G., Li, G., Sun, Y., Tao, B.: Intelligent human-computer interaction based on surface emg gesture recognition. *IEEE Access* **7**, 61378–61387 (2019)
  - [25] Schorr, S.B., Okamura, A.M.: Three-dimensional skin deformation as force substitution: Wearable device design and performance during haptic exploration of virtual environments. *IEEE Transactions on Haptics* **10**(3), 418–430 (2017)
  - [26] Tholey, G., Desai, J.P., Castellanos, A.E.: Force feedback plays a significant role in minimally invasive surgery: results and analysis. *Annals of surgery* **241**(1), 102 (2005)
  - [27] Van Kuilenburg, J., Masen, M.A., van der Heide, E.: A review of fingerpad contact mechanics and friction and how this affects tactile perception.

- Proceedings of the Institution of Mechanical Engineers, Part J: Journal of Engineering Tribology **229**(3), 243–258 (2015)
- [28] Vigotsky, A.D., Halperin, I., Lehman, G.J., Trajano, G.S., Vieira, T.M.: Interpreting signal amplitudes in surface electromyography studies in sport and rehabilitation sciences. *Frontiers in Physiology* p. 985 (2018)
- [29] Xydias, N., Kao, I.: Modeling of contact mechanics and friction limit surfaces for soft fingers in robotics, with experimental results. *The International Journal of Robotics Research* **18**(9), 941–950 (1999)
- [30] Zheng, M., Crouch, M.S., Eggleston, M.S.: Surface electromyography as a natural human–machine interface: a review. *IEEE Sensors Journal* **22**(10), 9198–9214 (2022)